A Stacked Neural Network Approach for Yield Prediction of Propylene Polymerization

Seyed Ali Monemian,[1] Hamed Shahsavan,[2] Oberon Bolouri,[1] Shahrouz Taranejoo,[1] Vahabodin Goodarzi,[1] Mahmood Torabi-Angaji[1]

[1]*School of Chemical Engineering, University of Tehran, Tehran, Iran*
[2]*Chemical and Petroleum Engineering Department, Sharif University of Technology, Tehran, Iran*

Received 13 April 2008; accepted 7 August 2009
DOI 10.1002/app.31251
Published online 23 December 2009 in Wiley InterScience (www.interscience.wiley.com).

ABSTRACT: Prediction of reaction yield as the most important characteristic process of a slurry polymerization industrial process of propylene has been carried out. Stacked neural network as an effective method for modeling of inherently complex and nonlinear systems–especially a system with a limited number of experimental data points–was chosen for yield prediction. Also, effect of operational parameters on propylene polymerization yield was modeled by the use of this method. The catalyst system was $Mg(OEt)_2$/DIBP/$TiCl_4$/PTES/$AlEt_3$, where $Mg(OEt)_2$, DIBP (diisobutyl phthalate), $TiCl_4$, PTES (phenyl triethoxy silane), and triethyl aluminum ($AlEt_3$) (TEAl) were employed as support, internal electron donor (ID), catalyst precursor, external electron donor (ED), and co-catalyst, respectively. The experimental results confirmed the validity of the proposed model. © 2009 Wiley Periodicals, Inc. J Appl Polym Sci 116: 1237–1246, 2010

Key words: stacked neural network; modeling; polyolefins; Ziegler–Natta polymerization

INTRODUCTION

Ziegler-Natta catalysts are the most common and important commercial catalyst systems to produce millions of tons of polyethylene and polypropylene to fulfill strong worldwide demand. A considerable proportion of this demand is met by large scale, slurry and gas phase processes. Supported catalysts enable us to use high activity polymerization systems with negligible reactor fouling, and at the same time, producing polymer powders of good morphology and high bulk density.

To obtain a better polymerization behavior, traditional supports such as MgO,[1] $Mg(OH)_2$,[2] $MgCl_2$,[3] and silica[4] have been used; but among them, silica and $MgCl_2$ have received the most attention and are being used immensely in olefin polymerization. As simple silica supported catalysts have not been able to polymerize polypropylene successfully,[5] magnesium compounds (especially $MgCl_2$) have been known to be the most useful supports. But high hygroscopicity of $MgCl_2$ and high chlorine content of $MgCl_2$ supported catalysts make its use difficult. Thus, some studies have been conducted to improve catalyst preparation methods by use of the Magnesium Alkoxides to obtain good polymerization behaviors. As a result, the chemical reaction method for preparation of such catalysts using a $Mg(OEt)_2$/ID/TEAl/$TiCl_4$/ED system have appeared to result in the most favorable polymerization behavior.[6–9]

There are only a few records reporting a comprehensive review on the effect of operational parameters on polymerization of propylene to get suitable productivity and isotacticity index (I.I.%);[10–13] therefore, a thorough study on the effect of operational parameters on the mentioned systems would be useful. According to the fact that process modeling is proved to be successful in many facets of process engineering and it can be utilized to reach predictive purposes, modeling of such a system would be valuable. As industrial processes behave nonlinearly in some cases, developing of an accurate model for control, optimization, and simulation would be a difficult task. Artificial neural network (ANN) is known as one of effective methods, capable of modeling of inherent complex and nonlinear systems.[14]

Recently, in some papers focused on the polymerization process, the effects of the variables and operating conditions on the final polymer properties and productivity have been investigated with assistance of artificial intelligence.[15–19]

Among the ANN techniques, stack generalization is a technique for combining neural networks in order to provide a practical model for prediction. To improve the accuracy of model, especially when limited numbers of experimental data points are

Correspondence to: M. Torabi-Angaji (mtorabi@ut.ac.ir).

TABLE I
Catalyst Elemental Analysis Results

Element	Wt % in Catalyst 1	Wt % in Catalyst 2
Ti	2.75	2.6
Mg	22.01	21.8
Cl	58.01	55.36

available, stacked neural network (SNN) is recommended.[20] As we knew from literature survey, despite its unique characteristics, there is no report within the literature utilizing SNN technique in polymerization processes.

In this article, $Mg(OEt)_2$ supported catalyst was prepared and characterized. A comprehensive study on the effect of operational parameters on the polymerization behavior of the synthesized catalyst has been implemented. Finally, the effect of the process variables on the polymerization yield was investigated through the proposed SNN model.

EXPERIMENTAL SECTION

Chemicals

Magnesium ethoxide and phenyl triethoxy silane were purchased from Fluka (Switzerland). DIBP, $TiCl_4$, and toluene (extra pure grade) were purchased from Merck (Germany). A 1 *M* solution of TEAl was supplied from Schering (Germany). Propylene and nitrogen (99.999% purity) were prepared from Arak Petrochemical (Iran). Normal heptane and *n*-hexane ($[H_2O] < 3$ ppm) were supplied from Shazand Refinery (Iran).

Preparation of catalyst

$Mg(OEt)_2$ (10 g) and $TiCl_4$ (20 mL) were added to 80 mL dried toluene in a 200 mL three-necked flask vigorously stirring with a magnetic stirrer under nitrogen pressure. Upon reaching 90°C, 2.7 mL DIBP was added as internal donor (ID). The reaction was continued for 2 h at 115°C. After decantation, product of the reaction was washed at 40°C two times and each time with 100 mL dried toluene. The same process was carried out at 115°C for another 2 h and treated in 80 mL toluene with 20 mL of excess amount of $TiCl_4$. On completion of the process, the catalyst was washed 10 times with *n*-hexane at 80°C and dried under nitrogen pressure. Finally, the mixture of 2 g of washed catalyst and 40 mL of dried *n*-heptane was located under the nitrogen purge to be injected into polymerization reactor.

Typical polymerization procedure

Polymerization was conducted in a 1.6 L Buchi type reactor equipped with a mechanical stirrer (adjusted to 500 rpm during the polymerization).

After removing all the moisture, air, and impurities by purging with nitrogen, the reactor was charged with 800 mL *n*-heptane. Co-catalyst was injected into the reactor 5 min after the injection of external donor (ED) solution. Then, catalyst suspension was injected into the reactor and stayed in contact with mixture of co-catalyst and ED solutions. The preparation of co-catalyst and ED was done by addition of 10 mL of 1 *M* solution TEAl to 63.3 mL and 24 mL of PTES to 76 mL of *n*-heptane, respectively. Finally, solvent was saturated with monomer and warmed upto the desired reaction temperature and supplied with continuous pressure at the ambient polymerization pressure. The monomer line was always set to 10 bar and could be regulated to another pressure level for a different polymerization condition. At the end of polymerization process, produced polymer was weighted after being filtered and dried in vacuum at 70°C.

Catalyst and polymer characterization

Ti and Mg content of the catalyst were determined by atomic adsorption spectrophotometer (Shimadzu 6800). 100–150 mg of the catalyst dissolved in 10 mL of 0.2*N* sulfuric acid and diluted to 100 mL with distilled water. Chlorine content was measured by Volhard's method.[21,22] Chemical microstructure of the catalyst was obtained by FTIR with an 8 : 1 (w : w) ratio mixture of catalyst to potassium bromide using

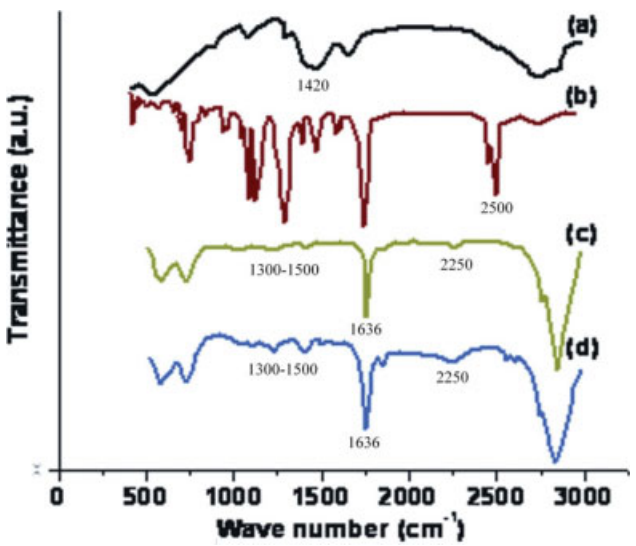

Figure 1 FTIR spectra of: (a) $Mg(OEt)_2$, (b) DIBP, (c) Catalyst 1, and (d) Catalyst 2. [Color figure can be viewed in the online issue, which is available at www.interscience.wiley.com.]

TABLE II
BET and Longmuir Specific Surface Area

Catalytic system	BET (m^2/g)	Longmuir (m^2/g)
Catalyst 1	270.71	938.20
Catalyst 2	244.81	770.30

Test Scan Series 8000 Shimadzu. Specific surface area of the catalyst was measured via BET method. Extraction of precipitated isotactic polymer in boiling normal heptane was used to calculate percentage of isospecifity of the polymer as discussed in the literature.[23]

Elemental analysis

Table I tabulates elemental analysis for a sample of the synthesized catalysts (Catalyst 1). The results were compared with an industrial $Mg(OEt)_2$ supported catalyst donated by Arak Petrochemical. (Catalyst 2). The results obtained from the synthesized catalysts are comparable with the industrial one.

FTIR analysis

FTIR analysis enables us to recognize catalyst chemical structure. Figure 1 shows the resultant spectra. As it is shown in both catalysts spectrum [Fig. 1(c,d)], the peak at 1420 cm^{-1}, appearing to correspond to $Mg(OEt)_2$, has shifted to 1636 cm^{-1}, corresponding absorbance band for $MgCl_2$.[13] It means that due to the reaction between ethoxide groups and $TiCl_4$, a great amount of ethoxide groups have been changed to $MgCl_2$. The weak peaks in the range 1300–1500 cm^{-1} are probably representative of different types of $Mg(OEt)_2$ or $TiCl_{4-n}(OEt)_n$ and the evidence for attendance of residual ethoxide groups in the form of $Mg(OEt)_2$ and $TiCl_{4-n}(OEt)_n$. The spectrum for DIBP shows a strong band at 2500 cm^{-1}, which is shifted to 2250 cm^{-1} in catalysts spectra.[24]

Specific surface area, porosity, density

Specific surface area of the catalyst was obtained from nitrogen absorption results at different relative pressure levels. According to the observed isotherms that are in concurrence with Bruner second type isotherms describing a multi-layer absorption behavior,[25] the best correlation for the measurement of these types is BET equation. BET calculation is based on multi-layer physisorption, whereas Longmuir calculation is based on the simple layer physical absorption. Table II compares the BET and Longmuir specific surface areas of Catalyst 1 and Catalyst 2. As it is obvious, magnificent increase in specific surface area was obtained in comparison with industrial catalyst and data from other investigations on fourth generation Ziegler-Natta catalyst in the literature.[26]

TABLE III
Average Pore Volume and Diameter

Catalytic system	Average pore volume	Average pore diameter
Catalyst 1	0.281	35.98
Catalyst 2	0.225	35.99

In majority of the studies, pore size distribution of the catalyst particles is obtained by considering the desorption branch of nitrogen adsorption isotherms. Here, this quantity was measured using BJH method. Table III shows average pore volume and average pore diameter for the Catalyst 1 and Catalyst 2.

TABLE IV
Bulk Density and Porosity

Catalytic system	Bulk density (g/cm^3)	Porosity
Catalyst 1	0.447	0.334
Catalyst 2	0.554	0.405

Table IV shows the porosity and bulk density results for the catalysts. It is apparent that the porosity of the Catalyst 2 is less than that of Catalyst 1.

Effect of operational parameters on propylene polymerization

In this section the effect of operational parameters on propylene polymerization using Catalyst 1 is investigated as follows:

Effect of co-catalyst/transition metal molar ratio

As it can be seen in Table V, catalyst activity increased in terms of the polymerization productivity until reached a maximum and then fell. It was found that the addition of Al-alkyl co-catalysts to the catalyst system and subsequently their interactions progressively activated the potential active sites and increased their number, resulting in increase of the polymerization productivity.[27–29] Also, study of different quantitative methods of

TABLE V
Effect of Al/Ti Ratio on Propylene Polymerization[a]

No.	Al/Ti (molar ratio)	Yield (Kg PP/(g Ti)[a]h)	I.I.%
1	330	66	98.3
2	440	68	98.1
3	520	70	97.5
4	740	80	97.1
5	850	58	96.8

[a] Polymerization conditions: [Ti] = 0.052 mmol/lit, P = 9 bar, T = 70°C, time = 2 h, agitator speed = 500 rpm

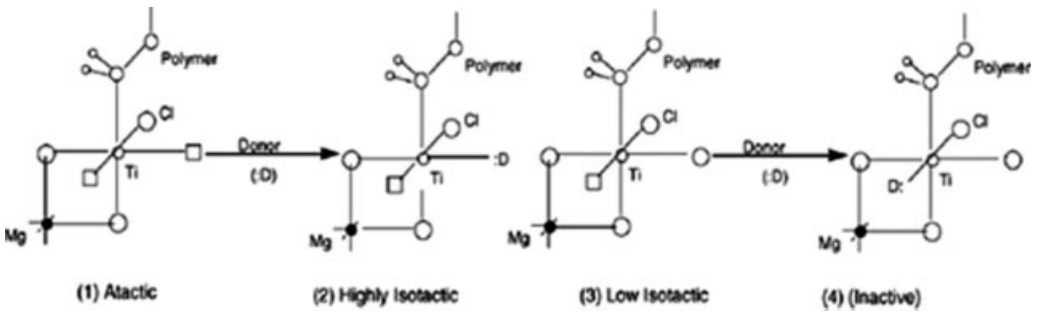

Figure 2 Models for the active centers on supported Ti catalyst and the effect of an ED; (□) Cl vacancy.[44]

determination of Ti^{n+} species in the catalyst system demonstrated that the majority (almost 90%) of initial Ti ions on the catalyst surface were of type Ti(IV) reduced to lower valence states such as Ti(III) and even Ti(II) due to alkylation with co-catalyst ligands.[30–35] Besides, industrial and scientific, records show that polymerization of propylene at the temperatures near 70°C with catalyst systems is similar to our system, a considerable amount of active sites are formed by species of oxidation states higher than Ti(II). In fact, for similar catalytic systems, the Ti(II) species are inactive to polymerize propylene.[31,36–38]

Therefore, considering the fact that reduction processes are fostered due to increase of Al-alkyl concentration, formed active sites may suffer from deactivation caused by over-reduction of titanium species form higher oxidation states like Ti(IV) and Ti(III) to inactive Ti(II) species during both catalyst/co-catalyst pretreatment and polymerization process.[35,39] Therefore, falling of catalyst activity as a result of this reality is expectable.

A slight decrease of I.I.% after use of higher concentrations of co-catalyst might be ascribed by removal/extraction of ID due to complexation with co-catalyst species, as it is reported in the literature.[39] Owing to the fact that the interaction between ID and Ti species is not very strong,[27,40] addition of higher amounts of co-catalyst might cause the extraction of a large amount of IDs by formation of complexes with TEAl, and finally resulting transform of isospecific Ti-ID complexes to specific uncomplexed Ti species.[39] This is likely the most reasonable theory to explain the effect of co-catalyst on I.I.% of the final polymer.

Effect of co-catalyst/ED ratio

It is well known that use of a Lewis bases as ED remarkably affects the stereospecifity, polymerization kinetics and the activity of Ziegler-Natta catalysts.[41,42]

It is found that addition of the ED to the catalyst systems improves the stereospecifity of the active sites by reversible complexation of it to the coordinatively unsaturated active sites.[43]

According to Kakugu et al.,[44] there are two kinds of active site structures in the first steps of the polymerization (a specific active site, which is labeled by structure 1 in Figure 2 and low-isospecific active site as labeled by structure 3).

They suggest that addition of ED improves the isospecifity of the catalyst due to transformation of a specific active centers of structure 1 to high isotactic active sites of structure 2, resulting in a remarkable increase in I.I.% of the final polymer. However, simultaneously transformation of structure 3 as a result of use of high amounts of ED may cause an activity decrease due to generation of inactive sites after transformation of low isotactic active sites to inactive ones under structure 4.

Table VI shows the obtained results from polymerization of the synthesized catalyst using different

TABLE VI
Effect of External Electron Donor on Propylene Polymerization

No.	Al/Si (molar ratio)	Yield (Kg PP/(g Ti)[a]h)	I.I.%
1	20	66.8	96.5
2	16	80	97.1
3	10	70	97.8
4	5	64	98.6

[a] Polymerization conditions: [Ti] = 0.052 mmol/lit, P = 9 bar, T = 70°C, time = 2 h, Al/Ti = 740, agitator speed = 500 rpm

TABLE VII
Effect of Monomer Pressure on Propylene Polymerization[a]

No.	Pressure (bar)	Yield (Kg PP/(g Ti)[a]h)	I.I.%
1	6	32	98.1
2	7	60.8	97.5
3	8	70	97.3
4	9	80	97.1
5	10	97	97

[a] Polymerization conditions: [Ti] = 0.052 mmol/lit, T = 70°C, time = 2 h, Al/Ti = 740, Al/Si = 16, agitator speed = 500 rpm

TABLE VIII
Effect of Temperature on Propylene Polymerization[a]

No.	Temperature (°C)	Yield (Kg PP/(g Ti)[a]h)	I.I.%
1	55	72	98.6
2	60	73.6	98.2
3	65	75.6	97.7
4	70	80	97.1
5	75	64	95.5
6	80	50	94.2

[a] Polymerization conditions: [Ti] = 0.052 mmol/lit, P = 9 bar, time = 2 h, Al/Ti = 740, Al/Si = 16, agitator speed = 500 rpm

amounts of ED in terms of Al/Si molar ratio. As it is obvious, the productivity of the catalyst increased to a maximum point and then fell because of an increase in number of inactive sites in higher amounts of ED. But I.I.% of product rose monotonically due to increase in ED amount. Lee et al.[27] have reported similar results similar to the observed trend.

Effect of monomer pressure

By choosing optimum amounts of ED and co-catalyst leading to the most polymerization productivity obtained in previous steps of experiments, and 70°C as the polymerization temperature, a slightly linear dependency of productivity to different pressures in the range 6–10 bar was being observed, as shown in Table VII. This was due to the fact that higher pressure and concentration of monomer causes catalyst particles to break (especially in initial steps of reaction) and to locate new created active centers in the polymerization media.[45,46]

Effect of temperature

Polymerization was carried out at different temperatures in the range 55–80°C. According to Table VIII, due to increase in temperature, activity rose to a maximum point and then began to fall. At high temperatures, diffusion is the determining step of polymerization rate. On the other hand, gas solubility in liquid at high temperatures decreases because of the increase of molecular kinetic energy of gas.[44] Also, that result might be ascribed to naturally irreversible destruction reaction of active centers takes place at high temperatures.[45]

Also, according to Table VIII a considerable decline of I.I.% for the final polymer took place with increasing the polymerization temperature. Similar results are observed in several reports.[27,37,47]

TABLE IX
Effect of Time on Propylene Polymerization[a]

No.	Time (h)	Yield (Kg PP/(g Ti)[a]h)
1	1	57.2
2	2	80
3	3	107.2
4	4	118
5	5	136

[a] Polymerization conditions: [Ti] = 0.052 mmol/lit, P = 9 bar, T = 70°C, Al/Ti = 740, Al/Si = 16, agitator speed = 500 rpm

TABLE X
Effect of Hydrogen on Propylene Polymerization

No.	H_2 (cm^3)	Yield (Kg PP/(g Ti)[a]h)	I.I.%
1	0	80	97.1
2	50	120	97.0
3	100	136	96.1
4	150	148	95.8
5	200	168	95.1

[a] Polymerization conditions: [Ti] = 0.052 mmol/lit, P = 9 bar, T = 70°C, time = 2 h, Al/Ti = 740, Al/Si = 16, agitator speed = 500 rpm

Effect of reaction time

Productivity rose with extending the polymerization time. Most of the polymer production took place at initial steps of reaction and at final step the rate fell noticeably according to Table IX.

Effect of hydrogen

In this section, the effect of addition of hydrogen during the polymerization process was studied. Hydrogen was used as a chain transfer unit to control the molecular weight of the polymer for the commercial production of polyolefins, such as PP and PE using Ziegler-Natta catalysts. In spite of the fact that the mechanism of the activation behavior and chain transfer reaction remains obscure,

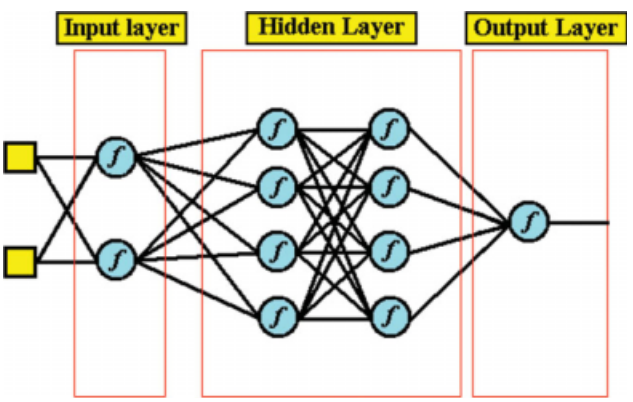

Figure 3 Schematic architecture of an ANN. [Color figure can be viewed in the online issue, which is available at www.interscience.wiley.com.]

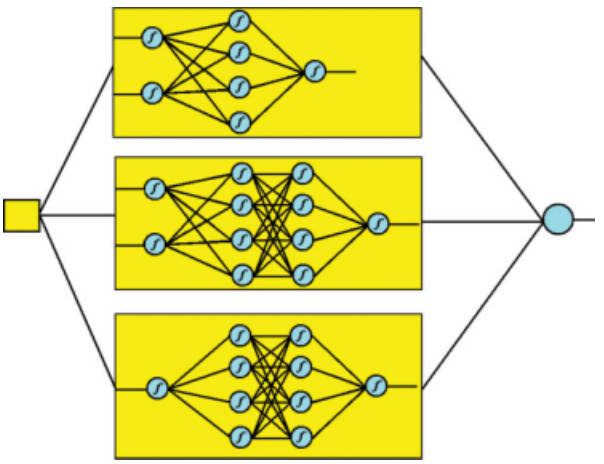

Figure 4 Schematic architecture of a SNN. [Color figure can be viewed in the online issue, which is available at www.interscience.wiley.com.]

majority of the studies introduce hydrogen as an activator, increasing polymerization rate and also controlling MW of the polymer. This reality emerges from the theory, in which activating effect of hydrogen can likely be ascribed to regeneration of active species following chain transfer with hydrogen at "dormant" 2, 1-inserted sites.[48–52] However, some studies show the detrimental effects of hydrogen for the rate of polymerization.[53] As monomer solubility in the polymer particle enhances as a result of introduction of hydrogen to the polymerization media, the rate of polymerization of propylene increases in the cases hydrogen as a chain transfer agent is used.[54] Also, it is demonstrated that hydrogen gas can be used for the purpose of controlling not only molecular weight but the molecular weight distribution of the polymer. The latter directly depends on the distribution of active species with different valence states on the catalyst surface. On the ground that hydrogen produces a variety of valence states for Ti on the catalyst surface due to continuous chain transfer reactions, an obvious change in polymerization rate in initial and declining periods of polymerization process occurs.[55,56]

According to Table X, addition of higher amounts of hydrogen resulted in increased activity of this catalytic system. In addition, it shows a sensible decrease in I.I.% of polymer in presence of higher amounts of hydrogen.

THEORETICAL SECTION

Artificial neural network

ANN is a computer based algorithm inspired by actual neurological system. It is made of interconnected elements called nodes or artificial neurons, which are a model of biological neurons. Depending on their application, many types of ANN architectures have been developed, such as, Kohonen, feed-forward, radial basis for applications, such as, self organizing map, pattern recognition, and function approximation.[57,58] It has been proven mathematically that feed-forward structure is a universal approximator.[59]

A simple Feed-forward ANN has three layers of neurons. The first layer is called input layer, which receives information from outside of the network. The second layer, where most of the calculation happens is known as hidden layer. It may have more than one layer depending on system complexity. Being hidden for user, the process performed in the hidden layer is known as black box. The last layer is called output layer, which receives processed information from network and sends the result to an external receptor.[60] Figure 3 shows a four layer feed-forward neural network with 2,4,4,1 neurons in input, hidden, and output layers, respectively.

Each neuron receives information from its interconnected neurons by its weight factor and calculates the output by its transfer function or activation function (F) as follows:

$$\mathrm{Out} = \mathrm{F}\left(\sum_{\mathrm{i}=1}^{\mathrm{n}} (\omega_{\mathrm{i}} \mathrm{x}_{\mathrm{i}}) + \mathrm{b}\right) \quad (1)$$

where x_i is input data, ω_i is weight factor for ith data, n is number of input data, and b is bias. F could be hyperbolic tangent, sigmoid, linear, Gaussian function, etc.

To have an ANN capable of producing desired results, its parameters i.e., ω_i and b should be determined to minimize the error between experimental data and produced data. Thus, learning algorithm is applied to train ANN. Many learning algorithms have been developed, such as, Conjugate Gradient, Levenberg-Marquardt (LM), and Bayesian learning. Among them, LM algorithm performs faster.[61] To train ANN, dataset is divided in two parts. One of them is for training the network and the other is for

TABLE XI
Statistical Analysis to Assess the Prediction Performance for level-0 Models

Level-0 model	ANN1	ANN2	ANN3	ANN4	ANN5
SSE	0.35252	0.75357	0.97634	0.13566	0.64352

TABLE XII
Statistical Analysis to Assess the Prediction Performance for Level-1 Model

Method	Average	Weighted average	ANN
SSE	0.57232	0.14692	0.00923

testing the trained network. The success in making a robust ANN relies strongly on the choice of the process variables as well as dataset used for training. There are situations during training process, in which the training error reduces while the testing error is still rather high. This is called overfitting. To avoid overfitting, two methods have been suggested; one is regularization and the other is early stopping. The latter is used in this study. In this method, another dataset is created besides training and testing datasets called validation dataset.[62] Training process will stop if validation error increases.

Modeling a system with ANN does not always guarantee the perfect prediction of the system. This could be due to trapping learning algorithm in local minima, design of neural network architecture or lack of enough experimental data. Thus, it built up the idea of combining neural networks and stack generalization.

Stacked neural network (SNN)

Stack generalization is a technique for combining neural networks in order to provide a practical model for prediction. To improve the accuracy of model, when limited numbers of experimental data points in training dataset are available, SNN is recommended.[20] In this method, several types of ANN models are combined in order to improve model performance. Figure 4 shows a simple architecture of SNN.

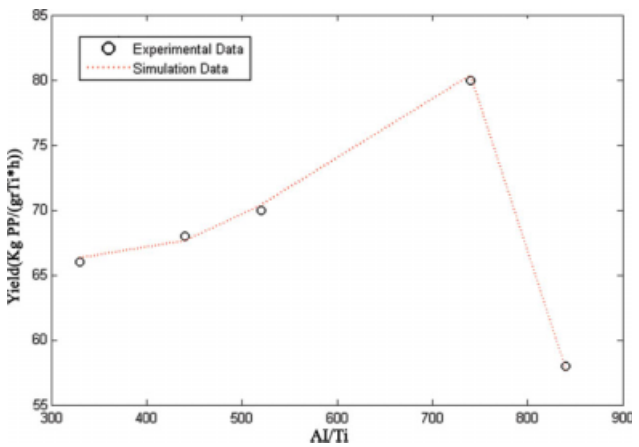

Figure 5 Prediction of the effect of Al/Ti variation on yield by SNN and its comparison with the experimental data. [Color figure can be viewed in the online issue, which is available at www.interscience.wiley.com.]

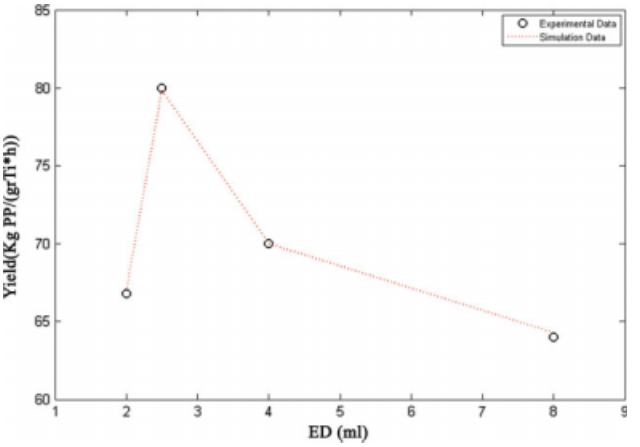

Figure 6 Prediction of the effect of ED variation on yield by SNN and its comparison with the experimental data. [Color figure can be viewed in the online issue, which is available at www.interscience.wiley.com.]

ANN models developed from original dataset are called level-0 models. For a brief overview of this technique, suppose that there are two level-0 models. Original datasets are divided in two subsets. Both level-0 models are designed, trained with first subset and tested by the other one so that the perfect architecture with minimum error between desired output and calculated output is developed. The output of these level-0 models along with the original output data forms a new dataset. This dataset is then used for modeling of higher level of the stacked structure i.e. level-1 model.[63]

There are several approaches to develop a level-1 model. A simple approach is to take equal weight factor for each individual level-0 model.[64] Second way is to combine weighted output of each individual level-0 model presented by the following equation:

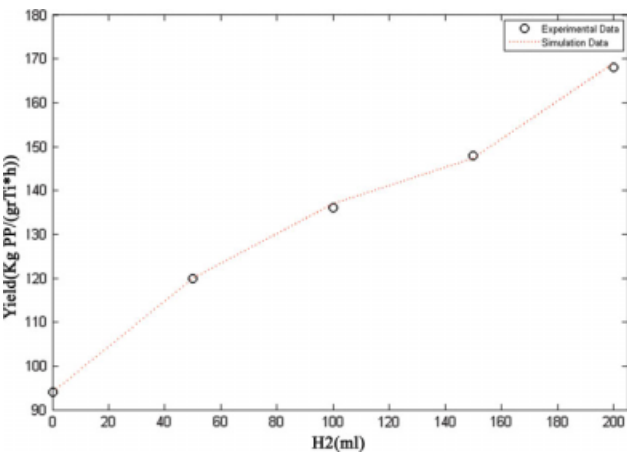

Figure 7 Prediction of the effect of H_2 variation on yield by SNN and its comparison with the experimental data. [Color figure can be viewed in the online issue, which is available at www.interscience.wiley.com.]

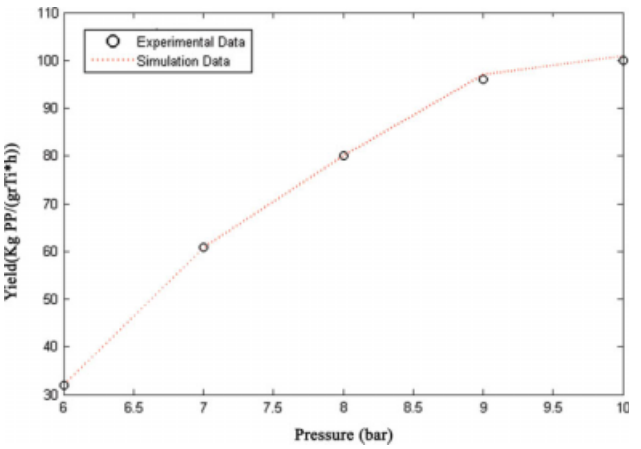

Figure 8 Prediction of the effect of pressure variation on yield by SNN and its comparison with the experimental data. [Color figure can be viewed in the online issue, which is available at www.interscience.wiley.com.]

$$Y(X) = \sum_{i=1}^{n} (\omega_i y_i(X)) \quad (2)$$

where Y is output of SNN, X is vector of ANN input data, n is number of ANN models, and ω_i is weight factor for combining the ith ANN set by principal component regression (PCR).[64] Third approach is combining the models by using principal component analysis (PCA), where output from level-0 models are used as training data to train a new level-1 ANN model.[20]

In this article, five ANN models were developed as level-0 model with different architecture and different subset of experimental data. The experimental dataset was divided in five different subsets. The first ANN model was designed and trained with first subset and then tested with the next one. This procedure was repeated until satisfactory error between desired output and calculated output was obtained. In this way, the best architecture for current network was found. The same procedure was used to design other four ANN models. All the networks were trained by LM algorithm with early stopping criteria to avoid overfitting. For each ANN, 80% of subset was used for training and the rest 20% was used for cross validation. Accuracy evaluation of all ANN models was based on sum of square error (SSE) between desired output and calculated output. To develop the ANN models, number of nodes in each hidden layer and number of hidden layers were varied as well as number of training and testing data in subsets.

Therefore, five level-0 models were developed. A couple of them had one hidden layer with three nodes (ANN1, ANN2). Another couple of them had one hidden layer with five nodes (ANN3, ANN4) and the last level-0 model had two hidden layers with three nodes (ANN5). All level-0 models had sigmoid, hyperbolic tangent and linear activation functions in their input, hidden, and linear output layers, respectively. Output of these level-0 models along with the original experimental data formed a new dataset for level-1 model.

RESULTS AND DISCUSSION

Results obtained from yield prediction for all five level-0 models are presented in Table XI. For level-1 model, three mentioned methods for developing a SNN model were applied and the results are presented in Table XII. As shown in Table XII, among these three methods, error of simple average method is the highest. Error of weighted average method is lower than simple average method because each individual connection weight is considered in this

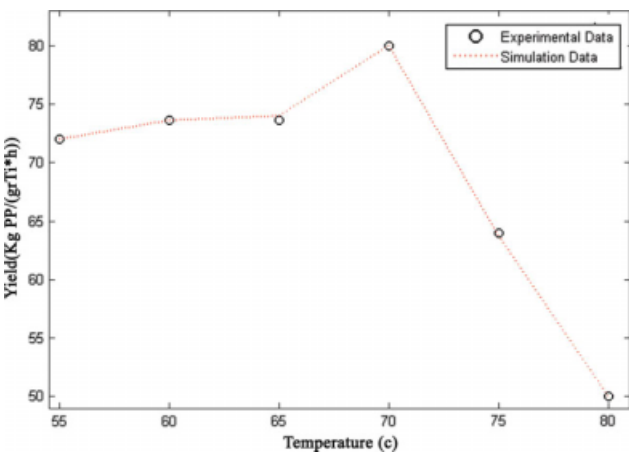

Figure 9 Prediction of the effect of temperature variation on yield by SNN and its comparison with the experimental data. [Color figure can be viewed in the online issue, which is available at www.interscience.wiley.com.]

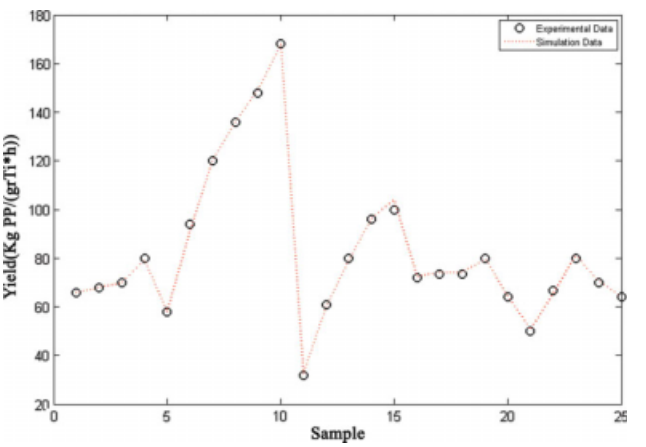

Figure 10 Evaluation of the SNN model accuracy. [Color figure can be viewed in the online issue, which is available at www.interscience.wiley.com.]

approach. ANN model as third approach shows the best result due to training and learning from level-0 data.

By comparing SSE values in Tables XI and XII, it is observed that though SSE values for level-0 models were not satisfactory, SNN provided the best performance.

A case study on the effect of operational parameters on propylene polymerization was performed. The performance of SNN model to predict the limited numbers of experimental data is illustrated in Figures 5–9. As it is observed, the experimental data shows pretty good matches with the calculated data for the all studied operational parameters.

Figure 10 shows yield prediction and its comparison with the experimental data. It is shown that for limited amount of experimental data, SNNs developed a model considered as an acceptable yield prediction.

CONCLUSION

A fourth generation Ziegler-Natta catalyst was prepared via chemical reaction method. The effect of operational parameters on polymerization of the propylene polymerization was studied. The obtained results showed that there was an optimum molar ratio of Al/Ti to obtain the highest yield of polymer i.e., [Al]/[Ti] = 740. The highest activity of the catalyst was obtained at about 70°C. Increasing the monomer pressure from 6 to 10bar, increased the productivity of catalyst, monotonically.

Using a SNN modeling approach to predict the polymerization yield, the effect of operational parameters on slurry propylene polymerization was studied. Statistical analysis was performed to judge on accuracy of the model. Results obtained from this study showed that the predicted data were matched well with the experimental data. The proper result suggests that similar models can be used to estimate the yield of the complex and nonlinear processes versus the process variables.

References

1. Ivanchev, S. S.; Baulin, A. A.; Godianov, A. G. J Polym Sci Polym Chem Ed 1980, 18, 2045.
2. Kashiva, N.; Tokuda, T.; Fuimura, H. (Mitsui Petrochem Ind Ltd). Jpn. Pat. 7,040,295 (1970).
3. Kashiva, N.; Toyota, A.; Odawara, K. (Mitsui Petrochem Ind Ltd). Belg. Pat. 839,131 (1976).
4. Luo, H. K.; Tang, R. G.; Gao, K. J Catal 2002, 210, 328.
5. Lu, H.; Xiao, Sh. Makromol Chem 1993, 194, 421.
6. Job, R. C. (Shell Oil Co). US Pat. 4,535,068 (1985).
7. Kim, L.; Choi, H. K.; Kim, J. H.; Woo, S. I. J Appl Polym Sci 1994, 52, 1739.
8. Terano, M.; Kataoka, T.; Hasaka, M. (Toho Titanum Co. Ltd.). Jpn. Pat. 62,121,006 (1986).
9. Terano, M.; Soga, H.; Kimura, K. (Toho Titanum Co. Ltd.). US Pat. 4,829,037 (1986).
10. Jeong, Y. T.; Lee, D. H. Makromol Chem 1990, 191, 1487.
11. Kang, K. K.; Lee, D. H.; Jeong, Y. T. In Catalyst Design for Tailor-Made Polyolefins; Soga, K., Terano, M., Eds.; Kodansha, Elsevier: Tokyo, 1994; 153.
12. Kang, K. K.; Kim, K. S.; Lee, D. H.; Jeong, Y. T. J Appl Polym Sci 2001, 81, 460.
13. Pater, J. T. M.; Weickert, G.; Van Swaaij, W. P. M. Chem Eng Sci 2002, 57, 3461.
14. Azlan Hussain, M. Artif Intell Engng 1999, 13, 55.
15. Zhang, J.; Morris, A. J.; Martin, E. B.; Kiparissides, C. Comp Chem Eng 1999, 23, 301.
16. Zhang, J.; Yang, Q.; Zhang, S.; Howell, J. Control Eng Pract 1998, 6, 581.
17. Hanai, T.; Ohki, T.; Honda, H.; Kobayashi, T. Comput Chem Eng 2003, 27, 1011.
18. Fernandes, F. A. N.; Lona, L. M. F.; Penlidis, A. Chem Eng Sci 2004, 59, 3159.
19. Shi, J.; Liu, X.; Sun, Y. Neurocomputing 2006, 70, 280.
20. Wolpert, D. H. Neu Net 1992, 5, 241.
21. Kong, K. K.; Shiono, T.; Leong, Y. T.; Lee, D. H. J Appl Polym Sci 1991, 71, 293.
22. Montaudo, G.; Lattimer, R. P. In Mass Spectroscopy of Polymers, 1st Ed.; CRC Press: Boca Raton, 2002.
23. Natta, G.; Corrandini, P.; Bassi, I. F.; Porri, L.; Lincei, A. A. N. Rend Cl Sci Fis Mat 1985, 24, 121.
24. Zohuri, G.; Ahmadjo, S.; Jamjah, R.; Nekoomanesh, M. Iran Polym J 2001, 10, 149.
25. Brunauer, S.; Deming, L. S.; Deming, W.; Teller, E. J Am Chem Soc 1940, 62, 1723.
26. Kuran, W. Principles of Coordination Polymerisation; Wiley: Chichester, 2001.
27. Lee, D. H.; Jeong, Y. T.; Soga, K.; Shiono, T. J App Polym Sci 1993, 47, 1449.
28. Doi., Y.; Murata., K.; Yano., K.; Keii., T. Ind Eng Chem Prod Res Dev 1987, 21, 580.
29. Fregonese, D.; Mortara, S.; Bresadola, S. J Mol Catal A: Chem 2001, 172, 89.
30. Kojoh, S.-i.; Kioka, M.; Kashiwa, N. Eur Polym J 1999, 35, 751.
31. Chien, J. C. W.; Weber, S.; Hu, Y. J Polym Sci, Part A: Polym Chem 1989, 27, 1499.
32. Zakharov, V. A.; Makhtarulin, S. I.; Poluboyarov, V. A.; Anufrienko, V. F. Makromol Chem 1984, 185, 1781.
33. Baulin, A. A. Polym Sci USSR 1980, 22, 205.
34. Huang, Y. H.; Yu, Q.; Zhu, S.; Rempel, G. L.; Li, L. J Polym Sci, Part A: Polym Chem 1999, 37, 1465.
35. Kashiwa, N.; Yoshitake, J. Makromol Chem 1984, 185, 1133.
36. Mori, H.; Hasabe, K.; Terano, M. Polymer 1999, 40, 1389. and refrences within it.
37. Wang, W.; Wang, L.; Chen, T.; Sun, T. X.; Wang, J. J.; Chen, X. J Mol Catal A: Chem 2006, 244, 146.
38. Nitta, T.; Liu, B.; Nakatan, H.; Terano, M. J Mol Catal A: Chem 2002, 180, 25.
39. Shiono, T.; Soga, K. In Transition Metal Catalyzed Polemrization, Ziegler-Natta and Metal Polemrization; Quirk, R. P., Ed.; Cambridge University Press: New York, 1988; p 266.
40. Ikeuchi, H.; Yano, T.; Ikai, S.; Sato, H.; Yamashita, J. J Mol Catal A: Chem 2003, 193, 207.
41. Spitz, R.; Babichon, C.; Duranel, L.; Guyot, A. In Catalytic Olefin Polymerization; Keii, T., Soga, K., Eds.; Kodansha: Tokyo, 1990; p 43.
42. Sacchi, M. C.; Forlini, F.; Tritto, I.; Locatelli, P.; Morini, G.; Noristi, L.; Albizzati, E. Macromolecules 1996, 29, 3341.
43. Sivals, A. A. J.; Kissin, Y. V. J Polym Sci Polym Chem Ed 1984, 22, 3739.
44. Kakugo, M.; Miyatake, T.; Naito, Y.; Mizunuma, K. Macromolecules 1988, 21, 314.

45. Webb, S. W.; Weist, E. L.; Chiovetta, M. G.; Laurence, R. L.; Conner, W. C. Can J Chem Eng 1991, 69, 665.
46. Kissin, Y. V.; Mezhikovsky, S. M.; Chirkov, N. M. Eur Polym J 1970, 6, 267.
47. Sergeev, S. A.; Bukatov, G. D.; Zakharov, A. Makromol Chem 1984, 185, 2377.
48. Chadwick, J. C.; Kessel, G. M. M. V.; Sudmeijer, O. Macromol Chem Phys 1995, 196, 1431.
49. Chadwick, J. C.; Morini, G.; Albizzati, E.; Balbontin, G.; Mingozzi, E.; Cristofori, A.; Sudmeijer, O.; Kessel, G. M. M. Macromol Chem Phys 1996, 197, 2501.
50. Bukatov, G. D.; Goncharov, V. S.; Zakharov, V. A. Macromol Chem Phys 1995, 196, 1751.
51. Kojoh, S.; Kioka, M.; Kashiwa, N.; Itoh, M.; Mizuno, A. Polymer 1995, 36, 5015.
52. Chadwick, J. C.; Morini, G.; Balbontin, G.; Mingozzi, I.; Albizzati, E.; Sudmeijer, O. Macromol Chem Phys 1997, 198, 1181.
53. Soga, K.; Shiono, T. Polym Bull 1982, 8, 261.
54. Wu, Q.; Wang, H.; Lin, S. Macromol Chem Phys 1996, 191, 155.
55. Ha, K.; Yoo, K.; Rhee, H. K. J Appl Polym Sci 2001, 79, 2480.
56. Tannous, K.; Soares, J. B. P. Macromol Chem Phys 2002, 203, 1895.
57. Moradkhani, H.; Hsu, K. L.; Gupta, H. V.; Sorooshian, S. J Hydrol 2004, 295, 246.
58. Kalteh, A. M.; Hjortha, P.; Berndtsson, R. Environ Model Soft 2008, 23, 835.
59. Hornik, K.; Stinchcombe, M.; White, H. Neu Net 1989, 2, 359.
60. Baughman, D. R.; Liu, Y. A. Neural Networks in Bioprocessing and Chemical Engineering; Academic Press: San Diego, CA, 1995; p 508.
61. Hagan, M. T.; Menhaj, M. IEEE Trans Neu Net 1999, 5, 989.
62. Kim, T. Y.; Oh, K. J.; Kimc, C.; Do, J. D. Neurocomputing 2004, 61, 439.
63. Ghorbani, A. A.; Owrangh, K. International Joint Conference on Neural Networks (IJCNN'2001), Melbourne, Australia, 2001; p 1715.
64. Zhang, J.; Martin, E. B.; Morris, A. J.; Kiparissides, C. Comput Chem Eng 1997, 21, 1025.